Journal of Orthopaedic Translation 28 (2021) 74–82

Contents lists available at ScienceDirect

Journal of Orthopaedic Translation

journal homepage: www.journals.elsevier.com/journal-of-orthopaedic-translation

The construction of a novel xenograft bovine bone scaffold, (DSS) 6-liposome/CKIP-1 siRNA/calcine bone and its osteogenesis evaluation on skull defect in rats

Gang Xu [a,b], Xiantong Hu [c,d], Liwei Han [c,d], Yantao Zhao [c,d,**], Zhonghai Li [a,b,*]

[a] Department of Orthopaedics, First Affiliated Hospital of Dalian Medical University, Dalian, 116011, PR China
[b] Key Laboratory of Molecular Mechanism for Repair and Remodeling of Orthopaedic Diseases, Liaoning Province, Dalian, 116011, PR China
[c] Department of Orthopaedics, Fourth Medical Center of PLA General Hospital, Beijing, 100048, PR China
[d] Beijing Engineering Research Center of Orthopaedic Implants, Beijing, 100048, PR China

ARTICLE INFO

Keywords:
Xenograft bone scaffolds
True bone calcine
casein kinase 2 interacting protein-1
siRNA
Bone defect

ABSTRACT

Background: Xenograft bone scaffolds have advantages such as mechanical strength, sufficient source and safety. Combined with siRNA properly targeting CKIP-1, a negative regulator of osteogenesis, may contribute to the repair result of calcine bone alone.
Methods: Herein, we constructed a novel xenograft bovine bone scaffold namely (DSS)6-liposome/CKIP-1 siRNA/calcine bone, the characteristics of which were investigated by confirming the effect of (DSS)6-liposome, observing the appearance and testing mechanical strength of calcine bone, and observing the combined result of CKIP-1 siRNA by FAM immunofluorescence. In addition, cytotoxicity by CCK-8 and LDH activity of L929 cells and MC3T3-E1 osteoblasts cultured with the scaffold were tested in vitro, primary osteoblasts proliferation, the mRNA expressions of CKIP-1, ALP, COL1-α and OCN, the protein expressions of CKIP-1, BMP-2, COL-1 and Runx2 and calcium nodules were also determined by CCK-8, RT-qPCR, western-blot and Alizarin Red staining in vitro. Then, we successively established the skull defect model for evaluating the repair result of the novel scaffold by HE staining of 2, 4, 8 and 12 weeks, immumohistochemical stainings of 2, 4, 8 and 12 weeks such as ALP, COL-1α and OCN, Mirco-CT scanning of 4 and 12 weeks and the relative parameters and so on in vivo.
Results: It indicated that (DSS)6-liposome/CKIP-1 siRNA/calcine bone could successfully knock down the CKIP-1 mRNA and protein expressions, promote osteoblasts proliferation with the little cytotoxicity in vitro, increase the protein expressions of BMP-2, COL-1 and Runx2 in vitro, increase mRNA expressions of ALP, COL-1α and OCN in vitro and in vivo, and have a better bone defect repair effect with few side effects in rats after 12 weeks.
Conclusion: Our research indicates (DSS)6-liposome/CKIP-1 siRNA/calcine bone could repair skull defects well in rats, and it may lay the foundation of applicating the novel xenograft bone scaffold in the clinical.
The Translational potential of this article: These findings provide evidence that (DSS)6- liposome/CKIP-1 siRNA/calcine bone could be used as a novel xenograft bone scaffold for osteogenesis with the good safety.

1. Introduction

As a kind of bone graft material with natural bone structure, xenograft calcine bone is made by degreasing and deproteinizing animal bone and then forging and burning at the high temperature. Its three-dimensional structure is very suitable for the growth of new bone. After the high temperature, its antigenicity can be completely eliminated, and immune rejection will not occur. It is rich in sources and the tissue, cell, blood compatibility and biological safety are also good. However, when it was implanted into organisms alone, it was difficult to become an ideal bone biological scaffold due to its limited surface area and lack of active factors [1,2]. The composite material can complement each other in terms of their properties. The preparation and application of composite material are currently active fields in the study of tissue engineering biomaterials, so calcined bone should be surface-modified in order to play a better role in osteogenesis [3,4].

* Corresponding author. Department of Orthopaedics, First Affiliated Hospital of Dalian Medical University, Dalian, 116011, PR China.
** Corresponding author. Department of Orthopaedics, Fourth Medical Center of PLA General Hospital, Beijing, 100048, PR China.
E-mail address: lizhonghaispine@126.com (Z. Li).

https://doi.org/10.1016/j.jot.2021.02.001
Received 10 July 2020; Received in revised form 23 January 2021; Accepted 1 February 2021

Casein kinase 2-interacting protein-1 (CKIP-1) is a protein that plays an important role in regulation of bone formation. The effect of CKIP-1 on bone formation is mainly mediated through negative regulation of the bone morphogenetic protein (BMP) pathway [5]. Recently, it has been reported that CKIP-1 could interact with Neuropilin-1 to suppress the odontoblastic differentiation of dental pulp stem cells via BMP2 pathway [6]. In addition, the deletion of CKIP-1in mice could alleviate the symptoms of osteoporosis induced by microgravity to some extent by affecting the process of bone formation [7], constrained dynamic loading and CKIP-1 gene knockout could counter unloading-induced bone loss, and combining the two treatments had an additive effect in mice [8], osteoblasts-targeting CKIP-1 siRNA treatment also attenuated the bone formation reduction in glucocorticoid induced osteoporosis mice [9], and local silencing CKIP-1 could promote bone formation through the Wnt3a/β-catenin signaling pathway in rat mandibular distraction osteogenesis [10]. Otherwise, the available in vivo bone-specific siRNA delivery system has been achieved involving dioleoyl trimethylammonium propane (DOTAP)-based cationic liposomes attached to six repetitive sequences of aspartate, serine, serine ((AspSerSer)6) (DSS)6 for silencing CKIP-1 [11]. Besides, a dual-functionalized graphene oxide based CKIP-1 siRNA delivery system had been established for implant surface bio-modification with enhanced osteogenesis [12]. Additionally, cross-species CKIP-1 siRNA sequences without immunostimulatory activity were identified [13]. The specificity of the action of CKIP-1 and the conservativeness of highly expressed tissues make CKIP-1 a preferred target for bone regeneration gene regulation therapy [14]. It has been reported a chitosan sponge incorporated small interfering RNA targeting CKIP-1 could also promote osteogenesis [15]. Chitosan/siCkip-1 biofunctionalized titanium implant could improve the osseointegration in the osteoporotic bilateral ovariectomy female rats [16]. However, the effect of xenograft calcine bone combined with small interfering RNA targeting CKIP-1 on bone defects is still unknown. Herein, we constructed a novel xenograft bovine bone scaffold, namely (DSS)6-liposome/CKIP-1 siRNA/calcine bone, to observe the osteogenesis for bone defects in rats.

2. Materials and methods

2.1. Bovine calcine bone preparation

The soft tissue of bovine bone was completely removed and it was cut into small pieces of 1 cm × 1 cm × 2 cm. The bone block was thoroughly cleaned with a high-pressure water gun, then treated with 0.5 mol/l NaOH solution and 3% H_2O_2 solution, and dried at 70 °C for 72 h. Then it was placed in a porcelain bowl, which was placed in a resistance furnace at room temperature and connected to an oxygen unit. The resistance furnace was heated at 10 °C/min, during which oxygen was continuously supplied. When the temperature rose to 500 °C, it was stopped for 30 min to prevent the carbonization and bursting of the bone block. When the temperature reached 850 °C, it was maintained for 4 h. After the bones were naturally cooled, they were placed in a pulverizer for grinding and powdering. The bone powder with a particle size of 270–1000 μm was screened and placed in a ziplock bag. After being sterilized by Co60 (25 kGy), it was stored in a refrigerator at 4 °C for use.

2.2. Loading of (DSS)6-liposome/CKIP-1 siRNA complexes

The (DSS)6-liposome was prepared according to the reference [11]. The CKIP-1siRNA (Sense: 5-GGACUUGGUAGCAAGGAAAdT*dT-3, Antisense: 5-UUUCCUUGCUACCAAGUCCdT*dT-3; according to the references [13], Shanghai GenePharma.) was incubated with the liposome at 1 μg: 1 ml for 20 min at room temperature, and the screened 1g calcined bone particles were added and combined overnight at room temperature. Then, 10% (w: w) sucrose was added and placed at 4 °C for 1 h, −18 °C for 12 h, −40 °C for 5 h, and then freeze-dried for 24 h. The compound efficiency could be detected by fluorescently labeled siRNA (FAM-siRNA) and quantitatively analyzed by Image-Pro Plus 6.0.

2.3. Cytotoxicity testing

Scaffolds were weighed and immersed in the α-MEM solution at 0.2 g/ml in a constant temperature incubator for 48 h to obtain the extraction solution of scaffolds. L929 cells (mice fibroblasts) or MC3T3-E1 osteoblasts were replaced with the extraction liquid of scaffolds. After the seventh day, 10 μl CCK-8 dye was added to the update culture medium for 4 h, detected at the wavelength of 450 nm. And the relative cells growth rate (RGR) was calculated to evaluate the cytotoxicity. ② After 72 h, the LDH activity was detected by the LDH kit and calculating the LDH cytotoxicity.

2.4. Real-time quantitative polymerase chain reaction

Total RNA was isolated from the cells using the TRIzol reagent. Then it was reverse-transcribed to the complementary DNA by RevertAid First Strand cDNA Synthesis Kit (Thermo Scientific Fermentas, Burlington, Canada). Real-time quantitative polymerase chain reaction (RT-qPCR) was performed as described previously [17]. Expression levels of CKIP-1, ALP, COL-1α and OCN (primers: referring to Refs. [10,13]) were corrected by normalization to the expression level of GAPDH, and relative expression levels were calculated with the $2^{-\Delta\Delta Ct}$ rule [18].

2.5. Western-blot

In a short word, protein samples from cells were separated by SDS-polyacrylamide gels, then transferred to PVDF membranes (0.45 μm) for the semiquantitative analysis. Membranes were blocked with 1% BSA T-TBS solution, then incubated with the primary antibodies (CKIP-1 antibody #sc-376060, BMP-2 antibody #sc-6895, COl-1 antibody #sc-59772 and Runx2 antibody #sc-390351, Santa Cruz Biotechnology, Inc., USA.), followed by incubation with the secondary antibodies conjugated with horseradish peroxidase. The antibody labelling was detected by ECL kit (Pierce) according to the manufacturer's instructions, and the images were put down by Gel analysis system (Tanon 5200 ECL Detection System, Tanon Science & Technology Co.).

2.6. Primary osteoblasts proliferation and differentiation

The primary rat osteoblasts were cultured according to our previous study [19]. Then, the primary cultured rat osteoblasts were seeded on the surface of the scaffolds (the thickness of 1 mm) at a certain density, 72 h later, cells proliferation was detected by CCK-8, the mRNA expressions of CKIP-1, ALP, COL1-α and OCN were detected by RT-qPCR, and the protein expressions of CKIP-1, BMP-2, COL-1 and Runx2 were detected by western-blot. And after 7 days, the primary cultured rat osteoblasts seeded on the surface of the scaffolds were stained by Alizarin Red and quantitatively analyzed by Image-Pro Plus 6.0.

2.7. Experimental animals

Experimental male CD-1 nude mice and male SD rats approved by the Animal Ethics Committee of the Fourth Medical Center of the PLA General Hospital. The environment was free of pathogens, the ambient temperature was 22 °C, 12 h light/12 h dark cycle was guaranteed every day, the indoor humidity was 50–55%, and adaptive feeding was carried out for one week before the experiment. NIH guidelines (or for non-U.S. residents similar national regulations) for the care and use of laboratory animals (NIH Publication #85-23 Rev. 1985) have been observed.

2.8. Bone induction in nude mice

The scaffolds were prepared into the same standard-size according to the same procedure, then implanted into the triceps muscle bags of bilateral hind limbs of nude mice, and the fascia layer and skin were sutured. The mice were randomly divided into A-D groups: calcine bone,

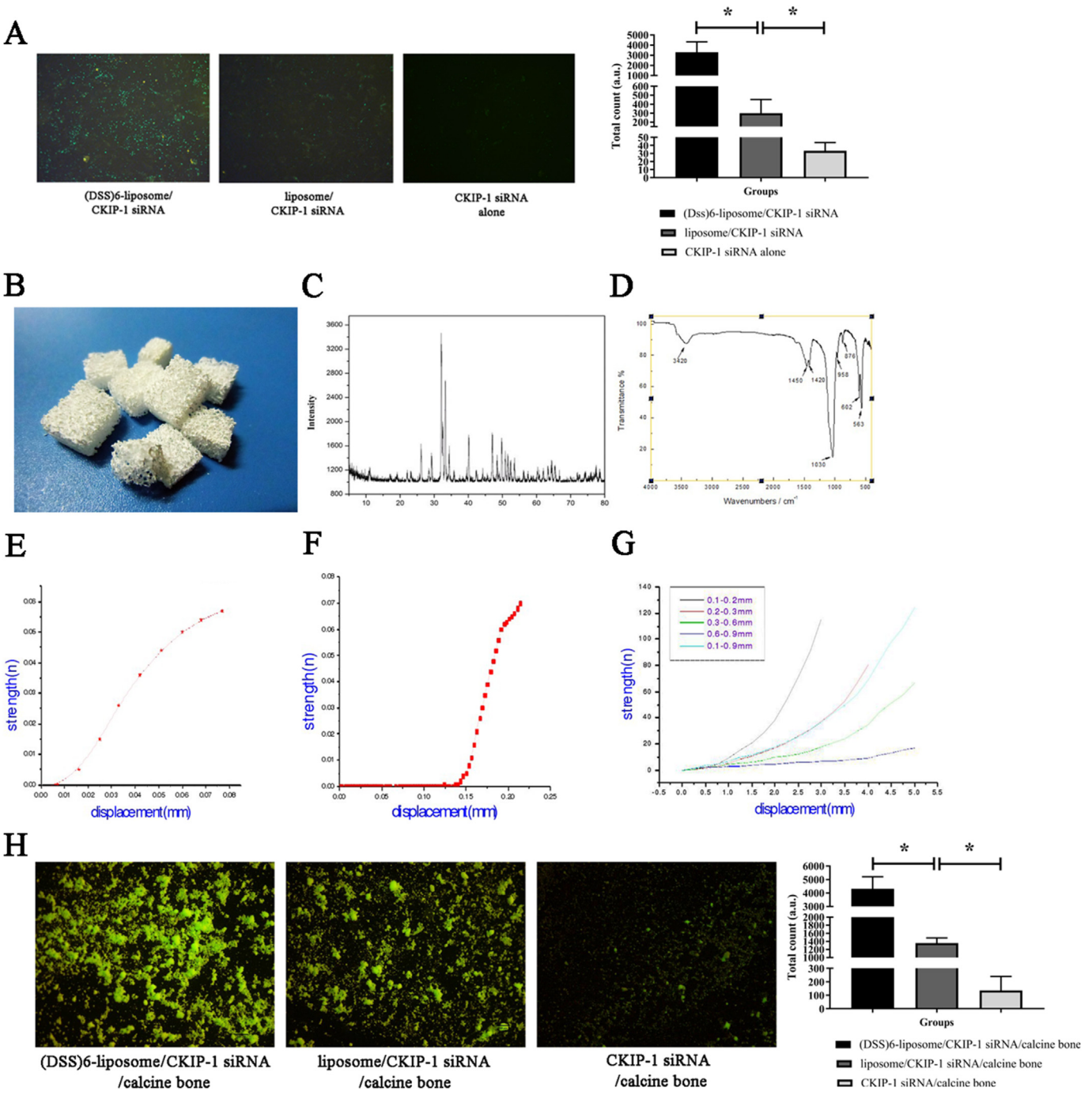

Figure 1. The construction of (DSS)6-liposome/CKIP-1 siRNA/calcine bone. A. FAM immunofluorescence modification, n = 3; B. The photograph of calcine bone; C. The XRD of calcine bone, n = 3; D. The IR of calcine bone, n = 3; E. The force and displacement curves of the spine ends of calcine bone, n = 3; F. The force and displacement curves of the spine middle of calcine bone, n = 3; G. The compressive strength of bone powder in different particle sizes, n = 3; H. The compound effect of calcined bone with CKIP-1 siRNA, n = 3.*P<0.05.

CKIP-1 siRNA/calcine bone, liposome/CKIP-1 siRNA/calcine bone, and (DSS)6-liposome/CKIP-1 siRNA/calcine bone. Hematoxylin-eosin (HE) staining was performed on scaffolds and the surrounding muscle tissues of postoperative 4 weeks to evaluate the osteoinductive activity of the scaffold.

2.9. Surgical procedures

Adult male SD rats weighing about 300 g were selected. The rats were anesthetized by intraperitoneal injection of 3% pentobarbital sodium, and were placed in the prone position. An incision of about 2 cm was made at the midline of the parietal skull to separate the periosteum, and a 5 mm diameter defect was made at the left and right sagittal suture with a bone trephine (Supplementary Fig 1 and 2). The scaffold was implanted into the defect and the periosteum and skin were sutured. Postoperative intramuscular injection of penicillin 80,000 units, continuous injection for 3 days, routine feeding. The operation was strictly aseptic and the defect was completed by the same group of researchers. The model rats were randomly divided into A-D groups: calcine bone, CKIP-1 siRNA/ calcine bone, liposome/CKIP-1 siRNA/calcine bone, and (DSS)6-

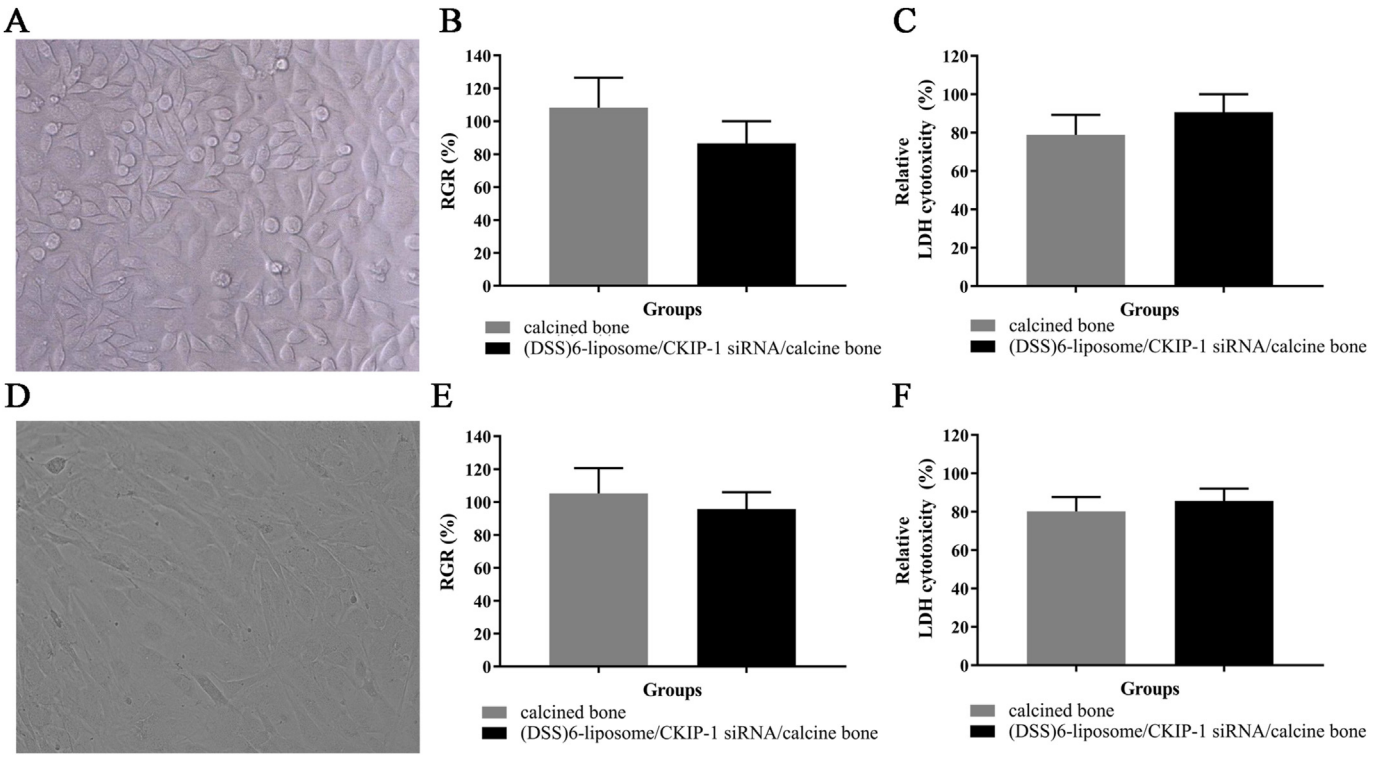

Figure 2. Cells activity and toxicity. A. The image of L929 cells; B. The relative L929 cells growth rate (RGR) by CCK-8 test, n = 5; C. The relative LDH cytotoxicity of L929 cells, n = 5. D. The image of MC3T3-E1 osteoblasts; E. The relative MC3T3-E1 osteoblasts RGR by CCK-8 test, n = 5; F. The relative LDH cytotoxicity of MC3T3-E1 osteoblasts, n = 5. *P<0.05.

liposome/CKIP-1 siRNA/calcine bone.

2.10. Histology analysis

HE staining

At the 2, 4, 8, 12 weeks after operation, the implant scaffolds and nearby bones were removed and immersed in 10% neutral buffered formalin fixative for fixation. After fixation, dehydration and decalcification, the cut surface was placed at the bottom for paraffin embedding, and sliced at a certain thickness, and then stained with HE for observation. The histological scoring criteria proposed by Nilsson were used [20]. Semi-quantitative analysis was performed by two experimenters who were unclear about the experimental group.

Immumohistochemical staining

At the 2, 4, 8, 12 weeks after operation, the implant scaffolds and nearby bones were removed and immersed in 10% neutral buffered formalin fixative for fixation. After fixation, dehydration and decalcification, the cut surface was placed at the bottom for paraffin embedding, and sliced at a certain thickness, and then were blocked and incubated with the primary antibodies of anti-ALP, anti-COL1α and anti-OCN (1:100, Santa Cruz Biotechnology, Santa Cruz, CA, USA) overnight at 4 °C. After incubation with the secondary antibodies (Santa Cruz) for 1 h at room temperature, the sections were washed and then visualized using diamino-benzidine. Staining quantity and intensity of positive cells were scored under a microscope in 3 randomly fields per slice. The scoring standard was referred to the reference [21]. Semi-quantitative analysis was performed by two experimenters who were unclear about the experimental group.

2.11. Micro-CT observation

After the fourth and eighth weeks, the skull was taken out from the rat. Micro-CT (Inveon MM CT) was used to scan and observe. Inveon Acquisition Workplace was selected as the scanning and analysis software.

2.12. Statistical analysis

GraphPad Prism 7.00 software were used for statistics and plotted. The measurement data were expressed as mean ± standard deviation. The statistical difference was tested by unpaired t-test or one-way ANOVA. P<0.05 indicated that there was a statistical difference.

3. Results

3.1. Construction and characterization of (DSS)6-liposome/CKIP-1 siRNA/calcine bone

Targeting molecule (DSS)6 (sequence: DSSDSSDSSDSSDSSDS SC5H8NO3S) was synthesised by Sangon Biological Engineering (Shanghai) Co., LTD. The quality control test report showed that it had high purity and its sequence could be coupled with liposomes (Supplementary Fig 3 and 4). FAM immunofluorescence modification was used to verify the transfection effect of (DSS)6-liposome/CKIP-1 siRNA, the transfection efficiency of (DSS)6-liposome was the highest, followed by the liposome alone and the siRNA alone in turn, as expected (Fig. 1A).

The calcine bone was shown as Fig. 1B. The porosity of calcine bone was 84.9% ± 0.6%, pore size distribution was between 200850 μm detected by SEM. The nitrogen content of the sample detected by metal sodium solution method was none, indicating no protein content. The main components of calcine bone were calcium phosphate and HA, detected by XRD (Fig. 1C) and IR (Fig. 1D). The bone density at both ends of the spine was 0.81–0.97 g/cm^3, and the compressive strength was 2.6–2.9 Mpa. The force and displacement curves were shown in Fig. 1E. The bone density in the middle part of the spine was 0.59–0.64 g/cm^3,

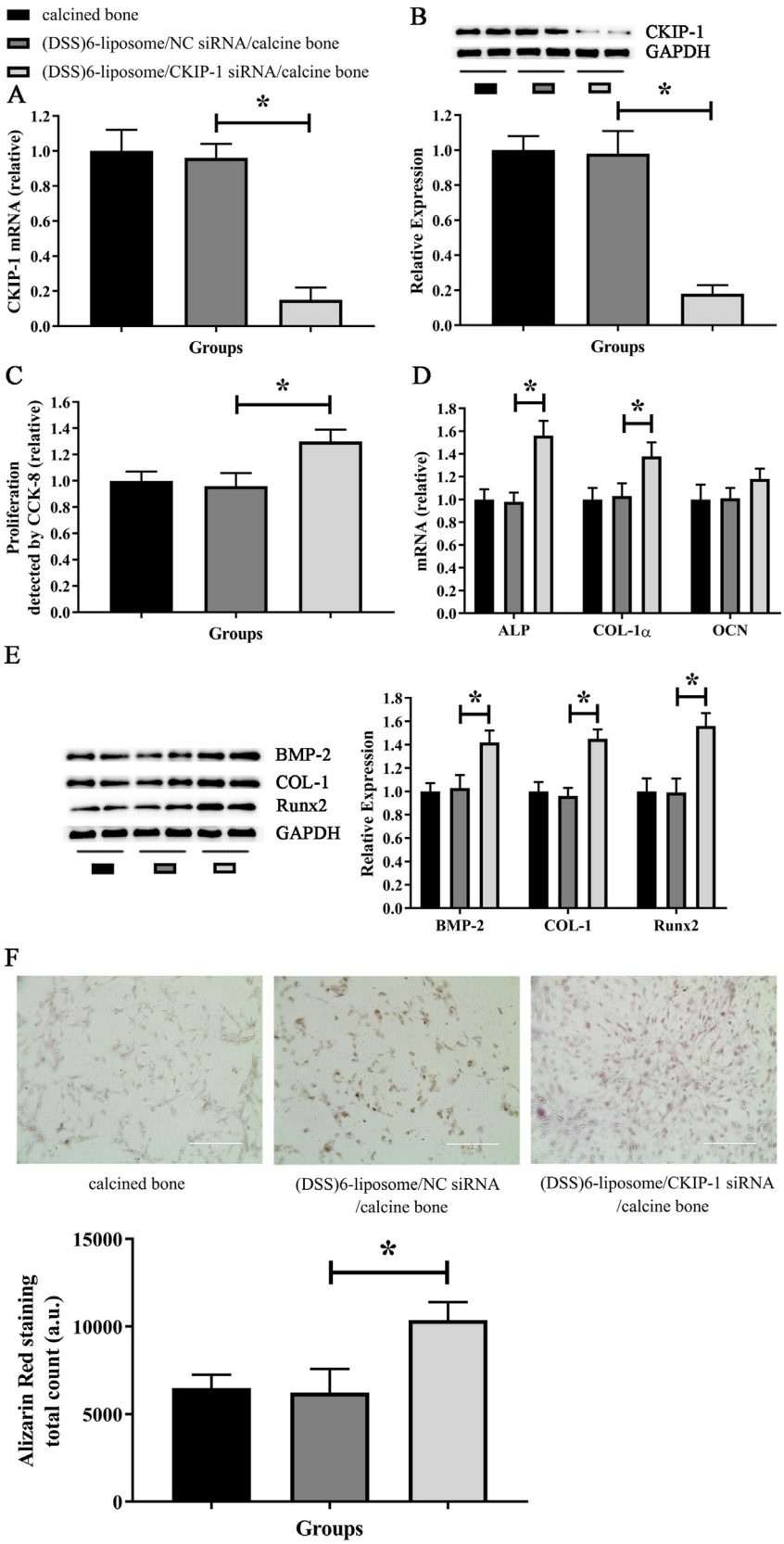

Figure 3. Osteoblasts proliferation and differentiation. A. The CKIP-1 mRNA expression, n = 3; B. The CKIP-1 protein expression, n = 4; C. The osteoblasts proliferation, n = 5; D. The mRNA expressions of ALP, COL1-α and OCN, n = 3; E. The protein expressions of BMP-2, COL-1 and Runx2, n = 4. F. Alizarin Red staining, n = 3. *$P<0.05$.

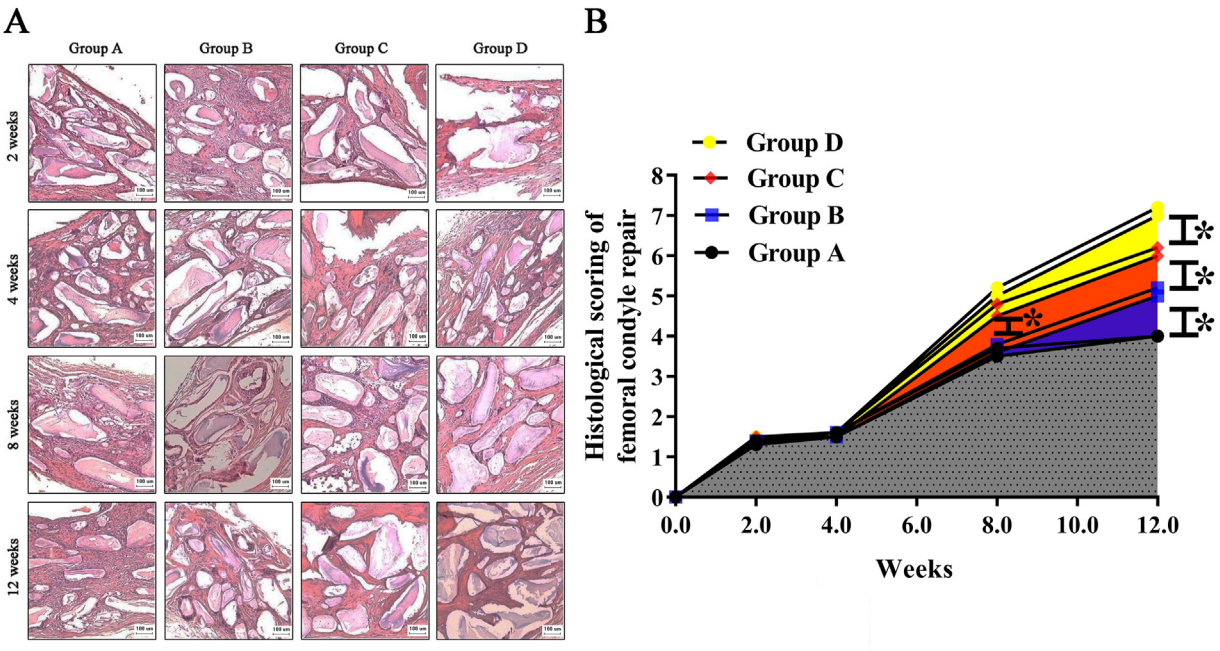

Figure 4. Pathological evaluation of defect repair. A. HE staining of 2, 4, 8 and 12 weeks; B. Histological scorings of 2, 4, 8 and 12 weeks, n = 2. *P<0.05. 200 μm, scale bar. A-D groups: calcine bone, CKIP-1 siRNA/calcine bone, liposome/CKIP-1 siRNA/calcine bone, and (DSS)6-liposome/CKIP-1 siRNA/calcine bone.

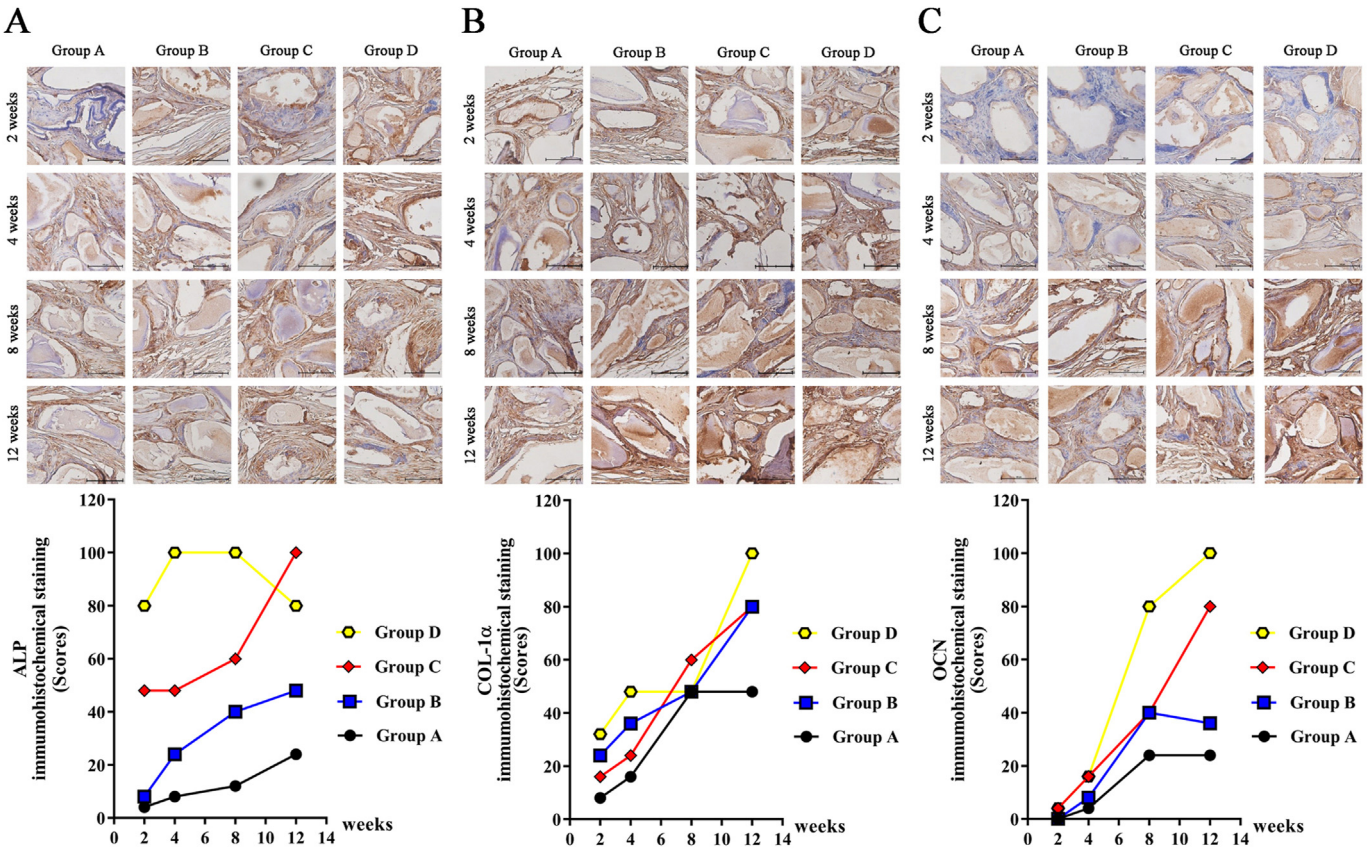

Figure 5. Immunohistochemistry analyze of osteoblast-related proteins. A. ALP staining of 2, 4, 8 and 12 weeks, and the histological scoring of 2, 4, 8 and 12 weeks, n = 3; B. COL1-α staining of 2, 4, 8 and 12 weeks, and the histological scoring of 2, 4, 8 and 12 weeks, n = 3; C. OCN staining of 2, 4, 8 and 12 weeks, and the histological scoring of 2, 4, 8 and 12 weeks, n = 3. *P<0.05. 100 μm, scale bar. A-D groups: calcine bone, CKIP-1 siRNA/calcine bone, liposome/CKIP-1 siRNA/calcine bone, and (DSS)6-liposome/CKIP-1 siRNA/calcine bone.

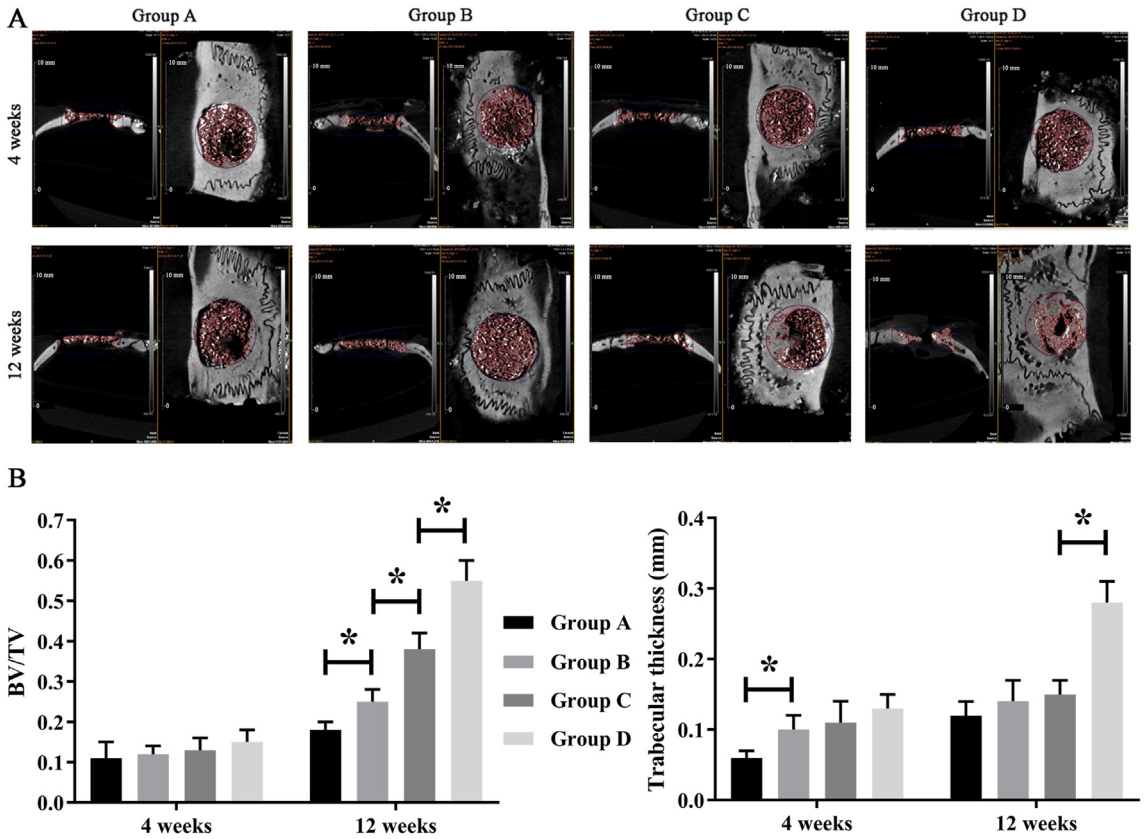

Figure 6. Micro-CT observation of defect repair. A. Micro-CT scanning of 4 and 12 weeks, n = 6; B. The bone mass/total volume (BV/TV) scores and the bone trabecular thickness, n = 6. *P<0.05. 10 mm, scale bar. A-D groups: calcine bone, CKIP-1 siRNA/calcine bone, liposome/CKIP-1 siRNA/calcine bone, and (DSS)6-liposome/CKIP-1 siRNA/calcine bone.

the compressive strength was 1.2–1.5 Mpa, and the force and displacement curves were shown in Fig. 1F. The compressive strength of bone powder in different particle sizes was shown as Fig. 1G. And the compressive strength of 0.10.9 mm, 0.10.2 mm and 0.20.3 mm was better than that of other groups. The compound effect of calcined bone with CKIP-1 siRNA was shown as Fig. 1H, (DSS)6-liposome/CKIP-1 siRNA was better than liposome/CKIP-1 siRNA, and the latter was also better than CKIP-1 siRNA alone.

3.2. Cells activity and toxicity

The cell morphology of L929 cells was spindle or polygon, with a full cell body and the large and clear, round or oval nuclei, and each cell contained 1 or 2 nucleoli. During the growth process, the cells were attached to adjacent cells and grow in flakes (Fig. 2A). The RGR by CCK-8 test of L929 cells cultured with calcine bone alone was higher than that of (DSS)6-liposome/CKIP-1 siRNA/calcine bone, however, the difference was not significant (Fig. 2B). Similarly, the relative LDH cytotoxicity of L929 cells cultured with calcine bone alone was lower than that of (DSS)6-liposome/CKIP-1 siRNA/calcine bone, and the difference was also not significant (Fig. 2C). In addition, MC3T3-E1 osteoblasts with the typical morphology (fusiform, triangular, or polygon with 1 or 2 nucleoli in each cell) (Fig. 2D) were also cultured to test the RGR and the relative LDH cytotoxicity. Consistent with the results of L929 cells, there were also no significant differences between calcine bone alone and (DSS)6-liposome/CKIP-1 siRNA/calcine bone (Fig. 2E and F).

3.3. Osteoblasts proliferation and differentiation

In primary rat osteoblasts, both the CKIP-1 mRNA (Fig. 3A) and protein (Fig. 3B) expressions of (DSS)6-liposome/CKIP-1 siRNA/calcine bone were obviously reduced than those of (DSS)6-liposome/NC siRNA/calcine bone or calcine bone alone, and the osteoblasts proliferation of (DSS)6-liposome/CKIP-1 siRNA/calcine bone was significantly promoted than that of (DSS)6-liposome/NC siRNA/calcine bone or calcine bone alone (Fig. 3C). Further, we also compared the mRNA expressions of ALP, COL1-α and OCN, which represented the osteogenesis differentiation, the mRNA expressions of ALP, COL1-α and OCN in the group of (DSS)6-liposome/CKIP-1 siRNA/calcine bone were all increased than those of (DSS)6-liposome/NC siRNA/calcine bone or calcine bone alone, while the OCN was not significant (Fig. 3D). In line with the above results, the protein expressions of BMP-2, COL-1 and Runx2 in the group of (DSS)6-liposome/CKIP-1 siRNA/calcine bone were also all increased than those of (DSS)6-liposome/NC siRNA/calcine bone or calcine bone alone (Fig. 3E). In addition, to ulteriorly confirm the osteoblast differentiation, Alizarin Red staining was performed and the result showed that (DSS)6-liposome/CKIP-1 siRNA/calcine bone had the better osteoblast differentiation than others (Fig. 3F).

3.4. Bone induction in nude mice

The results showed that there was no significant difference in osteogenic induction among the groups after 8 weeks (Supplementary Fig 5), indicating (DSS)6-liposome/CKIP-1 siRNA/calcine bone would not cause the ectopic ossification.

3.5. Pathological evaluation of defect repair

HE staining results showed that the repair of defects in each group at 2 weeks and 4 weeks was mainly about the coverage and filling of fibrous

tissue (Fig. 4A). At 8 weeks, bone repair began to occur in Group C and Group D, while the fiber repair was still dominant in Group A and Group B (Fig. 4A). At 12 weeks, a small amount of bone formation appeared in Group B, while a large amount of bone formation appeared in Group C and Group D. In Group A, fiber repair was still performed without osteogenesis (Fig. 4A). It indicated that both the scores and AUCs of Group C and Group D were improved after 8 weeks, with a statistical difference between Group B and Group C (Fig. 4B), and both the score and AUC of Group D were improved after 12 weeks, with a statistical difference between Group A, Group B, Group C and Group D ($P < 0.05$) (Fig. 4B).

3.6. Immunohistochemistry analyze of osteoblast-related proteins

Immunohistochemical results showed that COL-1α and OCN of four groups were expressed at a low level, ALP of Group C or D was expressed to some extent at 2 weeks indicating osteoblasts sooner migrated to the defect site. At 4 weeks, ALP and COL-1α began to express increasingly in each group, but the expression of OCN was not obvious in each group, implying osteoblasts were in the early stage of osteogenic differentiation without the expression of OCN. ALP and OCN were more expressed in Group D than those of other groups while COL-1α was expressed in each group nearly at the same level at 8 weeks, COL-1α and OCN were more expressed in Group D than those of other groups while ALP was most expressed in Group C at 12 weeks, exhibiting the middle and late osteogenic differentiation (Fig. 5A–C).

3.7. Micro-CT observation of defect repair

Micro-CT scanning was performed to compare the amount of new bone and percentage of bone formation 4 and 12 weeks after surgery (Fig. 6A). At 4 weeks, the BV/TV of all groups was nearly the same (Fig. 6B) while the trabecular thickness of Group A was obviously smaller than other groups (Fig. 6C). At 12 weeks, the BV/TV of Group D was significantly bigger than that of Group C, which of Group C was bigger than Group B, and Group B was also bigger than Group A (Fig. 6B). In the meantime, the trabecular thickness of Group D was obviously bigger than other groups (Fig. 6C).

3.8. Pathological evaluation of major tissues and organs

After 12 weeks, the rats were sacrificed and the main organs were taken: heart, liver, spleen, lung, kidney, brain and muscle. HE stainings were performed to observe the abnormal tissue morphology and evaluate the safety of the materials. The results showed that there were no obvious abnormalities in the main organs of the rats in each group (Supplementary Fig 6).

4. Discussion

Small interference RNA/calcined bone composite scaffold, a new type of gene intervention bone replacement holder, would inevitably face the safety test of siRNA in vivo experiments. After siRNA was introduced into the body, it was difficult to ensure that siRNA was pooled in the target tissue to play a therapeutic role locally. Due to the extensive presence of RNA degrading enzymes in body fluids, the structural integrity of small RNA could be destroyed in a short time, making it inactivated and completely degraded, which must be protected by carriers such as liposomes. In the study of siRNA, its effectiveness had been preliminarily understood and controlled, and the last barrier to the application of siRNA in vivo was the carrier system. Recent study found that (DSS) 6 had a special affinity of low crystallinity hydroxyapatite (HA), could obtain the solid combination effect of HA scaffold [11]. As the material was dissolved and degraded gradually after being implanted, (DSS) 6-liposome/CKIP-1 siRNA in local was also gradually released, under the action of the directional bond on osteogenesis interface of the low crystallinity HA, CKIP-1 siRNA would directly effect on the adjacent osteogenesis interface of osteoblasts and bone marrow stromal cells (BMSCs). HA in the new bone of osteogenesis interface presented the typical characteristic of the low crystallinity, then (DSS)6 with the affinity of low crystallinity HA could avoid the released CKIP-1 siRNA spreading throughout the body fluids a lot, instead, targeting the adjacent osteogenesis distribution area, which could be captured and utilized by the local osteogenesis interface and osteoblasts or BMSCs. After CKIP-1 siRNA entering cells, the function of local osteoblasts and BMSCs could be regulated to improve the local osteogenic activity and obtain better quality and strength of bone repair [6,9]. In agree with this point, the effect of CKIP-1 siRNA on the primary rat osteoblasts had also been investigated in vitro, and it indicated that (DSS)6-liposome/CKIP-1 siRNA/calcine bone could promote osteoblasts proliferation and increase the mRNA expressions of ALP, COL1-α and OCN and the protein expressions of BMP-2, COL-1 and Runx2, the actions mechanism of which should be related to the negative regulation of BMP pathway that had been reported [5,9]. Since the CKIP-1 siRNA did not affect the osteoclast activity and bone resorption, there was no simultaneous osteoclast effect. This was different from BMP [22–24].

The action time of siRNA transfected into cells in vitro was very short. Although the transfected cells usually showed a completely effective post-transcriptional silencing effect in a short time, the phenotype of this effect could be completely recovered after a few days, and the silencing effect disappeared. The usual siRNA gene silencing aging was 3–7 days. The active carrier could overcome the limitation of the short action time of siRNA silencing cells. Due to the continuous release of siRNA in the material with the degradation, the in-situ silencing of CKIP-1 protein could exert the effect of regulating osteogenesis and the formation of new bone with the continuous progress of material degradation. Therefore, on the basis of improving the physical and chemical properties of the composite scaffold, we attempted to compound (DSS)6-liposome/CKIP-1 siRNA with calcined bone scaffold, so as to promote its ability to repair bone defects. In our study, (DSS)6-liposome/CKIP-1 siRNA/calcine bone had the safety, histocompatibility and mechanical properties of in vivo implantation. There was no obvious abnormality in the main organs of rats in each group, which showed good safety. No obvious bone induction was observed in mice of each group indicating no ectopic ossification. The repair result of liposome/CKIP-1 siRNA/calcine bone was better than that of CKIP-1 siRNA/calcine bone or calcined bone alone, suggesting liposome/CKIP-1 siRNA/calcine bone also had the ability to repair the bone defects, with the improved rapid degradation of siRNA and osteogenesis to promote the healing of bone defects in vivo. Meanwhile, we found that the repair effect of (DSS)6- liposome/CKIP-1 siRNA/calcine bone was significantly better than that of other control scaffolds, indicating that it could further promote and accelerate the healing of bone defects. Moreover, recently, miR-98–5p targeted CKIP-1 by binding to its 3′-untranslated region presented the potential regulation of osteoblast differentiation in MC3T3-E1 pre-osteoblasts [25], reminding that miR-98–5p might play the same role to silence CKIP-1 instead of the siRNA and it could be our next work.

Taken together, we firstly reported (DSS)6- liposome/CKIP-1 siRNA/calcine bone, a novel xenograft bovine bone scaffold, could better promote and accelerate the healing of skull defects in rats, with the good safety. It may lay the foundation of applicating the novel xenograft bone scaffold in the clinical.

Funding

This study was supported by LiaoNing Revitalization Talents Program (XLYC1807131), the Natural Science Foundation of Liaoning Province (2019-BS-079), and the Science and Technology Innovation Foundation of Dalian (2020JJ27SN070), the National Natural Science Foundation of China(81672130), Military Medical Project (AWS14C007), Military Medical and Health Achievements Expansion Project (19WKS12). The funders had no role in the study design, data collection and analysis,

decision to publish, or preparation of the manuscript.

Declaration of competing interest

The authors declare no conflict of interest.

Acknowledgments

We would like to thank all the participants in the studies.

Appendix A. Supplementary data

Supplementary data to this article can be found online at https://doi.org/10.1016/j.jot.2021.02.001.

References

[1] Bracey DN, Cignetti NE, Jinnah AH, Stone AV, Gyr BM, Whitlock PW, et al. Bone xenotransplantation: a review of the history, orthopedic clinical literature, and a single-center case series. Xenotransplantation 2020:e12600.
[2] Song J, Kim J, Woo HM, Yoon B, Park H, Park C, et al. Repair of rabbit radial bone defects using bone morphogenetic protein-2 combined with 3D porous silk fibroin/β-tricalcium phosphate hybrid scaffolds. J Biomater Sci Polym Ed 2018;29(6):716–29.
[3] Noorjahan SE, Sastry TP. Physiologically clotted fibrin-calcined bone composite-a possible bone graft substitute. J Biomed Mater Res B Appl Biomater 2005;75(2):343–50.
[4] Zhang W, Li G, Deng R, Deng L, Qiu S. New bone formation in a true bone ceramic scaffold loaded with desferrioxamine in the treatment of segmental bone defect: a preliminary study. J Orthop Sci 2012;17(3):289–98.
[5] Lu K, Yin X, Weng T, Xi S, Li L, Xing G, et al. Targeting WW domains linker of HECT-type ubiquitin ligase Smurf1 for activation by CKIP-1. Nat Cell Biol 2008;10(8):994–1002.
[6] Song Y, Wang C, Gu Z, Cao P, Huang D, Feng G, et al. CKIP-1 suppresses odontoblastic differentiation of dental pulp stem cells via BMP2 pathway and can interact with NRP1. Connect Tissue Res 2019;60(2):155–64.
[7] Zhang X, Wang Q, Wan Z, Li J, Liu L, Zhang X. CKIP-1 knockout offsets osteoporosis induced by simulated microgravity. Prog Biophys Mol Biol 2016;122(2):140–8.
[8] Han B, Wei SP, Zhang XC, Li H, Li Y, Li RX, et al. Effects of constrained dynamic loading, CKIP-1 gene knockout and combination stimulations on bone loss caused by mechanical unloading. Mol Med Rep 2018;18(2):2506–14.
[9] Liu J, Lu C, Wu X, Zhang Z, Li J, Guo B, et al. Targeting osteoblastic casein kinase-2 interacting protein-1 to enhance Smad-dependent BMP signaling and reverse bone formation reduction in glucocorticoid-induced osteoporosis. Sci Rep 2017;7:41295.
[10] Zhou ZC, Che L, Kong L, Lei DL, Liu R, Yang XJ. CKIP-1 silencing promotes new bone formation in rat mandibular distraction osteogenesis. Oral Surg Oral Med Oral Pathol Oral Radiol 2017;123(1):e1–9.
[11] Zhang G, Guo B, Wu H, Tang T, Zhang BT, Zheng L, et al. A delivery system targeting bone formation surfaces to facilitate RNAi-based anabolic therapy. Nat Med 2012;18(2):307–14.
[12] Zhang L, Zhou Q, Song W, Wu K, Zhang Y, Zhao Y. Dual-functionalized graphene oxide based siRNA delivery system for implant surface biomodification with enhanced osteogenesis. ACS Appl Mater Interfaces 2017;9(40):34722–35.
[13] Guo B, Zhang B, Zheng L, Tang T, Liu J, Wu H, et al. Therapeutic RNA interference targeting CKIP-1 with a cross-species sequence to stimulate bone formation. Bone 2014;59:76–88.
[14] Peng X, Wu X, Zhang J, Zhang G, Li G, Pan X. The role of CKIP-1 in osteoporosis development and treatment. Bone Joint Res 2018;7(2):173–8.
[15] Jia S, Yang X, Song W, Wang L, Fang K, Hu Z, et al. Incorporation of osteogenic and angiogenic small interfering RNAs into chitosan sponge for bone tissue engineering. Int J Nanomed 2014;9:5307–16.
[16] Zhang L, Wu K, Song W, Xu H, An R, Zhao L, et al. Chitosan/siCkip-1 biofunctionalized titanium implant for improved osseointegration in the osteoporotic condition. Sci Rep 2015;5:10860.
[17] Zhou J, Xu G, Yan J, Li K, Bai Z, Cheng W, et al. Rehmannia glutinosa (Gaertn.) DC. polysaccharide ameliorates hyperglycemia, hyperlipemia and vascular inflammation in streptozotocin-induced diabetic mice. J Ethnopharmacol 2015;164:229–38.
[18] Livak KJ, Schmittgen TD. Analysis of relative gene expression data using real-time quantitative PCR and the 2(-delta delta C(T)) method. Methods 2001;25(4):402–8.
[19] Xu G, Zhao MJ, Sun N, Ju CG, Jia TZ. Effect of the RW-Cb and its active ingredient like P-acid and P-aldehyde on primary rat osteoblasts. J Ethnopharmacol 2014;151(1):237–41.
[20] Nilsson OS, Urist MR, Dawson EG, Schmalzried TP, Finerman GA. Bone repair induced by bone morphogenetic protein in ulnar defects in dogs. J Bone Joint Surg Br 1986;68(4):635–42.
[21] Friedrichs K, Gluba S, Eidtmann H, Jonat W. Overexpression of p53 and prognosis in breast cancer. Cancer 1993;72(12):3641–7.
[22] James AW, LaChaud G, Shen J, Asatrian G, Nguyen V, Zhang X, et al. A review of the clinical side effects of bone morphogenetic protein-2. Tissue Eng B Rev 2016;22(4):284–97.
[23] Sun SX, Guo HH, Zhang J, Yu B, Sun KN, Jin QH. BMP-2 and titanium particles synergistically activate osteoclast formation. Braz J Med Biol Res 2014;47(6):461–9.
[24] Niu H, Ma Y, Wu G, Duan B, Wang Y, Yuan Y, et al. Multicellularity-interweaved bone regeneration of BMP-2-loaded scaffold with orchestrated kinetics of resorption and osteogenesis. Biomaterials 2019;216:119216.
[25] Liu Q, Guo Y, Wang Y, Zou X, Yan Z. miR-98-5p promotes osteoblast differentiation in MC3T3-E1 cells by targeting CKIP-1. Mol Med Rep 2018;17(3):4797.